Efficient simulation from 3D tomographic images of heterogeneous materials

Xiaodong Liu, Julien Réthoré, Marie-Christine Baietto, Phillippe Sainsot, Ton Lubrecht

▶ **To cite this version:**

Xiaodong Liu, Julien Réthoré, Marie-Christine Baietto, Phillippe Sainsot, Ton Lubrecht. Efficient simulation from 3D tomographic images of heterogeneous materials. 14ème Colloque National en Calcul de Structures (CSMA 2019), CSMA, LEM3, MSME, Université de Lorraine, Arts et Métiers, CNRS, May 2019, Hyères, France. hal-04824594

HAL Id: hal-04824594
https://hal.science/hal-04824594v1

Submitted on 7 Dec 2024

HAL is a multi-disciplinary open access archive for the deposit and dissemination of scientific research documents, whether they are published or not. The documents may come from teaching and research institutions in France or abroad, or from public or private research centers.

L'archive ouverte pluridisciplinaire **HAL**, est destinée au dépôt et à la diffusion de documents scientifiques de niveau recherche, publiés ou non, émanant des établissements d'enseignement et de recherche français ou étrangers, des laboratoires publics ou privés.

CSMA 2019
14ème Colloque National en Calcul des Structures
13-17 Mai 2019, Presqu'île de Giens (Var)

Efficient simulation from 3D tomographic images of heterogeneous materials

X. Liu[1], J. Réthoré[1], M. C. Baietto[2], P. Sainsot[2];
A. A. Lubrecht[2]

[1] *GeM, Ecole Centrale Nantes, CNRS UMR 6183, {xiaodong.liu,julien.rethore}@ec-nantes.fr*
[2] *Univ Lyon, INSA-Lyon, CNRS UMR5259, LaMCoS, {marie-christine.baietto,philippe.sainsot,ton.lubrecht}@insa-lyon.fr*

Résumé — The use of tomographic images of materials as an input for numerical simulations is becoming more and more common. The main difficulty is the computational cost, mesh generations of finite element simulations and the large discontinuities of material properties. This work proposes a strategy to use a MultiGrid method coupled with homogenization techniques, with the help of parallel computing, to achieve a simulation of a tomographic image with more than 8 billion voxels at a low cost. Its effective property is also calculated.
Mots clés — Heterogeneous materials, MultiGrid, Homogenization, Effective property, Parallel computing

1 Introduction

The use of composite materials in many industrial fields has become more and more wide spread during the last decade. It is well known that many composite materials exhibit an excellent mechanical behavior. However, due to the complex structures and variable components of composite materials, it is not simple to understand their properties, which limits the application of these materials.

Fortunately, imaging techniques based on X-ray tomography show the inner structure of materials [1], which permits one to better understand the material behavior. Motivated by the secret of the material behavior, *e.g.* mechanical and thermal properties, using real tomographic images as an input to perform numerical simulations is under development. Much work has been devoted to this subject. The work of Lengsfeld *et al.* [2] and Bessho *et al.* [3] presented the numerical simulation of bone tomography. They studied mechanical problems *e.g.* hip fractures of the human femur, using Finite Element Methods (FEM). Ferrant *et al.* [4], Michailidis *et al.* [5] and Proudhon *et al.* [6] also applied FEM simulations to tomographic images of industrial materials to analyze their properties. As we saw previously, FEM is widely used for this kind of simulations. Nevertheless, the mesh generation of FEM needs human intervention, which is time consuming. The work of Gu *et al.* [7] introduced a 3D simulation of the elastic behavior of a laminated composite material. They proposed to use a Finite Difference Method (FDM), to take one voxel per grid point to avoid heavy human work in the meshing step, and to use the MultiGrid (MG) method to accelerate the convergence speed. However, the work of Gu *et al.* [7] can only deal with small size problems, due to the limitation of the serial programming. The fast fourier transform (FFT) is also a well known method, Nevertheless, it can not deal with problems with heterogeneity.

Motivated by these practical considerations, the development of a standard process to carry out numerical simulations on heterogeneous materials and to obtain its effective property, received considerable attention. The aim of this work is to take the tomographic image as an input to a thermal conduction simulation to study the material thermal behavior and to obtain its effective conductivity.

2 Problem statement

2.1 Governing Equations and iterative solver

Thermal conduction can be treated by a heat equation according to the first law of thermodynamics (*i.e.* conservation of energy) :

$$\rho c_p \frac{\partial T}{\partial t} - \nabla \cdot (\boldsymbol{\alpha} \nabla T) = \dot{q_v} \tag{1}$$

Since the focus of this work is thermal conductivity, it is considered that there is no extra source and the thermal field does not depend on time. The heat equation 1 becomes a typical Poisson equation :

$$\nabla \cdot (\boldsymbol{\alpha} \nabla T) = div(\boldsymbol{\alpha} \overrightarrow{grad(T)}) = 0 \tag{2}$$

The finite element discretization is chosen to disretize the domain Ω. The idea is to take one elementary node per voxel, to avoid the human intervention during the mesh generation step. A system of equations can finally be obtained :

$$\boldsymbol{L} \vec{T_h} = \vec{f} \tag{3}$$

where $\boldsymbol{L}$ is a matrix which is often referred to as the stiffness matrix, $\vec{T_h}$ is a vector containing all unknowns (temperature at each node) and $\vec{f}$ is the right hand side vector.

The largest image that will be computed in this application is an image containing 2049^3 voxels, which means that the number of elements is 2048^3 (*i.e.* more than eight billion elements). Supposing one uses cubic elements, the size of global sparse matrix is $2049^3 \times 27 \times 8\text{bytes} \approx 1.69$ TB. It is impossible to have such a huge memory space available on a normal computer. The size of the stiffness matrix does not allow one to assemble the whole matrix. It forces one to use an iterative solver without assembling the stiffness matrix, which is often called the Matrix Free Finite Element Method (MF-FEM) [8]. A Jacobi type MF-FEM iterative solver is therefore developed.

2.2 MultiGrid method and homogenization techniques

The single level Jacobi solver can only eliminate high frequency error for a large scale problem, it does not have a good convergence performance. As a consequence, the MultiGrid (MG) method is used to increase the convergence rate. Nevertheless, a standard MG method is not adapted for problems with high heterogeneity. It has a very poor convergence performance, when large variations of the material properties are to be considered. These variations make the linear interpolation and restriction operators almost ineffective. The coarse grid operator is also inefficient by this discontinuity.

Several researches have investigated this problem ([9], [10], [11] and [12]). These researchers proposed several methods to alleviate the poor convergence of the standard MG method. But the problem is that the implementation of these ideas is not simple. The computational time and memory cost are the two other limitations. In this work, the interpolation and restriction operator are developed based on the work of Alcouffe *et al.* [9]. For the coarse grid operator, Sviercoski *et al.* [13] proposed a Cardwell and Parsons (CP) bounds type homogenization to get the analytical coarse grid operator. The idea is to compute the upper and lower CP bounds of the material property on each coarse grid always from the finest grid, the average of the arithmetic and geometric averages of the CP bounds, is supposed to be the effective property on each coarse grid.

The weak point of the work of Sviercoski *et al.* [13] is the time consuming. Instead of the CP bounds type homogenization, one proposes to use a typical Voigt-Reuss (VR) bounds, which can be computed recursively. The material property $\boldsymbol{\alpha^H}$ on each coarse grid can be obtained by :

$$\boldsymbol{\alpha^H} = \frac{1}{2}(\boldsymbol{\alpha^a} + \boldsymbol{\alpha^g}) \tag{4}$$

where $\boldsymbol{\alpha^a}$ and $\boldsymbol{\alpha^g}$ are the arithmetic and geometric averages of the VR bounds. The coarse grid operator on each level can be easily obtained by the equation below :

$$L_H = \int_\Omega \nabla \phi_i^H \bar{\boldsymbol{\alpha}}^{\boldsymbol{H}} \nabla \phi_j^H \, d\Omega \tag{5}$$

where, ϕ_i^H and ϕ_j^H are test functions on each coarse grid.

3 Results

3.1 MG scheme efficiency

The performance of the MG scheme is studied by a simulation of a spherical thermal inclusion with a material property contrast of 10. The domain Ω is a cube with 128^3 elements. The relation between the radius r of the sphere and the size L of cubes is $r = \frac{L}{4}$. The simulation is run on an office computer equipped with one processor "Intel(R) Core(TM)2 Quad CPU Q9650 @ 3.00GHz".

	Single level	V-cycle MG scheme
Time used	2 **days** (48h)	84 **minutes**
Residual achieved	3.76×10^{-2}	3.99×10^{-6}
Number of cycles	1168 iterations	10 V-cycles

TABLE 1 – Comparison between single level relaxation and a MG scheme

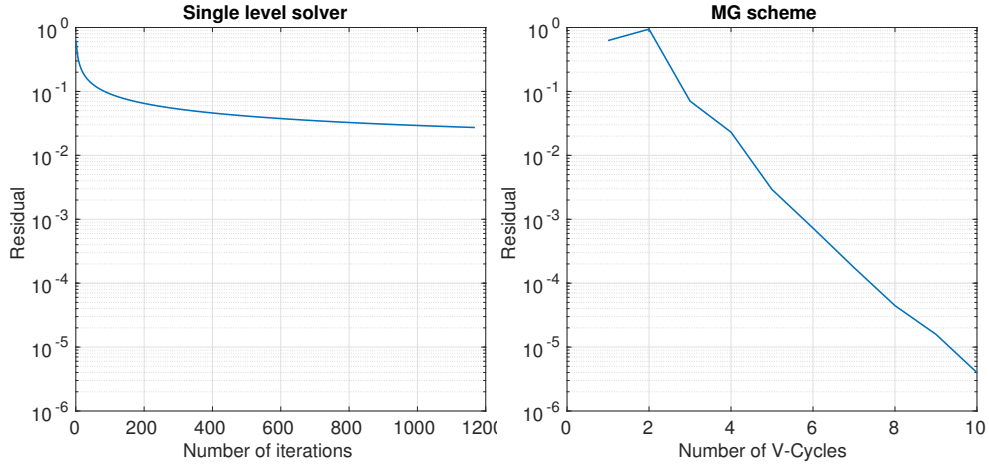

(a) Single level (b) MG scheme

FIGURE 1 – Convergence of the Jacobi solver (a) and MG scheme (b) on a 129^3 nodes problem

Table 1 and figure 1 illustrate the performance of the MG scheme compared to a single level Jacobi solver. The convergence rate of the single level Jacobi solver decreased rapidly. On the other hand, the convergence rate of the MG scheme remains constant. The MG scheme can obtain a residual 10 000 times smaller than that of the single level Jacobi solver, with a cost that is 34 times lower.

3.2 Parallel computing performance

As mentioned above, the goal of this work is the simulation of a domain discretized by more than eight billion elements, with a single processor, the computational time and memory are a big challenge. Suppose one uses the desk computer mentioned above, besides the memory limitations, a problem of eight billion elements (*i.e.* 4096 times larger than the previous one), will theoretically take about 239 days (*i.e.* 84×4096 minutes). The parallel computing is therefore necessary. MPI and OpenMP are the two mainly used parallel programming, to study their performance, a composite thermal conduction problem with more than 10^9 elements is applied.

The available supercomputer is a computer with 12 cores per processor and two processors per node, the number of cores can be used for one job is limited at 1 000 by the owner of this supercomputer. It is clear that the OpenMP code suffers from poor data access patterns when it uses two sockets, its performance decreases tremendously. The number of MPI per node is therefore defined at 2, and the number of OpenMP that can be used per MPI is 12.

The performance of number of OpenMP per MPI is firstly studied. Since the problem is too large, the number of MPI is fixed to 32 to reduce to computational time. As Figure 2a illustrates, 12 OpenMP

per MPI gives a full access at the available resource.

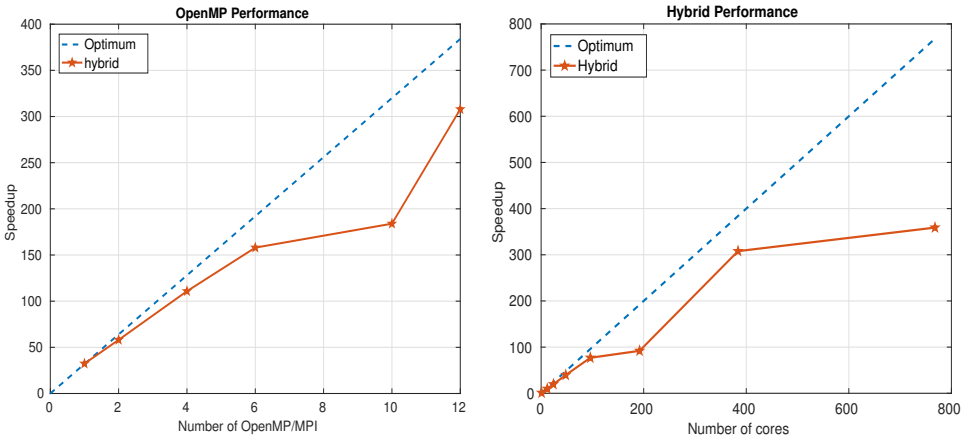

(a) OpenMP performance (b) Hybrid programming performance

FIGURE 2 – Parallel computing performance on a 10^9 elements problem

The performance of hybrid program is also tested. Figure 2b presents the speedup in function of the number cores used. As presented from 1 core to 384 cores, a good speedup is obtained. However, with 768 cores, the speedup is just a little larger than that with 384 cores. For a fixed problem, the percentage of the parallel parts is fixed, when increasing the number of cores, it can have a limitation. So a problem of 10^9 element, 384 cores is enough to have a best speed up considering the computational cost.

3.3 Effective conductivity of a layered composite material

Layered composite materials, which are widely used in the industrial domain due to its good performance, can be an anisotropic material. Employing numerical simulations directly on tomographic images can be good alternative to know the composite properties. The homogenization RVE is used to obtain the effective material property at the macroscopic scale.

The image used in this work is the image of a laminate composite material consisting of unidirectional E-glass fibers and a M9 epoxy matrix. It is a Glass Fiber Reinforced Polymer (GFRP) manufactured by the Hexcel Company. Its mechanical properties have been studied [14]. In this work, the heat transfer in this GFRP is studied to obtain its effective conductivity.

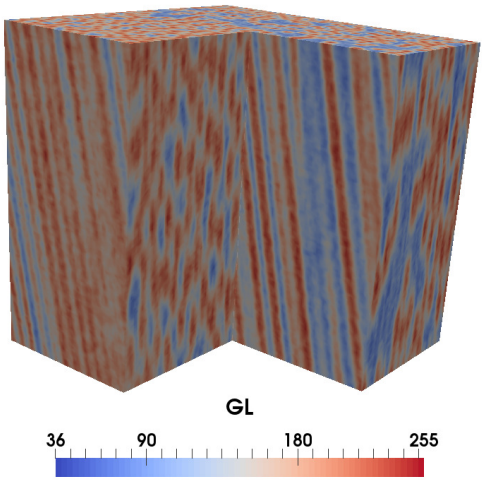

FIGURE 3 – ROI of the GFRP

The original image of this GFRP is an image consisting of $700 \times 1300 \times 1700$ voxels, As mentioned in the work of [14], this material is designed with four layers, the orientation of fibers is $+15°$,$-15°$,$-15°$ and $+15°$, respectively, for each layer. The idea is to take a cubic domain from the part which has the

same fiber orientation. One takes 129^3 voxels from the part with a fiber orientation of $-15°$, as the ROI (see Figure 3). As presented in Figure 3, the interface between the E-glass fiber and M9 epoxy matrix is not extraordinarily sharp. It is difficult to distinguish between these two phases (matrix and fiber). Instead of applying two discontinuous phases, one proposes to apply a continuous conductivity between 0.150 $\mathrm{W{\cdot}m^{-1}{\cdot}\,K^{-1}}$ (epoxy) and 1.30 $\mathrm{W{\cdot}m^{-1}{\cdot}\,K^{-1}}$ (E-glass fiber). One chooses to smooth the image gray level before it is used to compute the local material property at each voxel. It can be described as :

$$\alpha = 0.575\left(\left(1-e^{-\frac{|GL-160.5|}{20}}\right)sign\left(GL-160.5\right)+1\right)+0.15 \tag{6}$$

where GL is the original value of each voxel obtain by X–Ray tomography, which is an integer between 0 and 255. Except for the problem of the allocation of the conductivity, another problem is that the diameter of fiber is too small to have enough voxels in it. Sub-sampling *i.e.* linear interpolation, is therefore applied to this ROI to have more voxels in each fiber. The FEM discretization error therefore needs to be analyzed, to obtain the number of voxels needed for each section. A simulation with $\nabla\theta_x = 1$ $\mathrm{W{\cdot}m^{-1}{\cdot}\,K^{-1}}$ and $T = \nabla\theta_x x$ on $\partial\Omega$ is performed. The one time sub-sampling is applied to the ROI, the size of Ω is therefore 256^3 elements. Figure 4 illustrates the conductivity of each node in this ROI after one time sub-sampling.

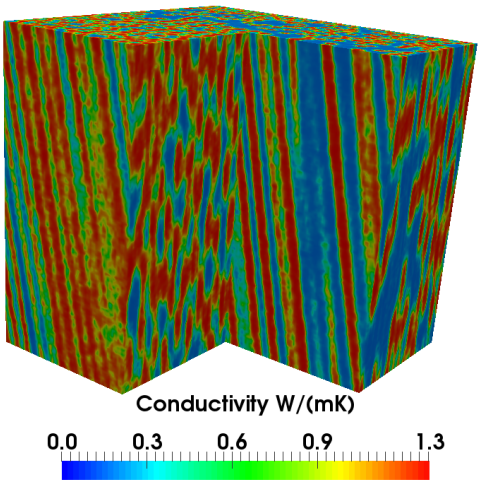

FIGURE 4 – GFRP conductivity

The temperature gradient is computed, as presented in Figure 5. The effective conductivity of the

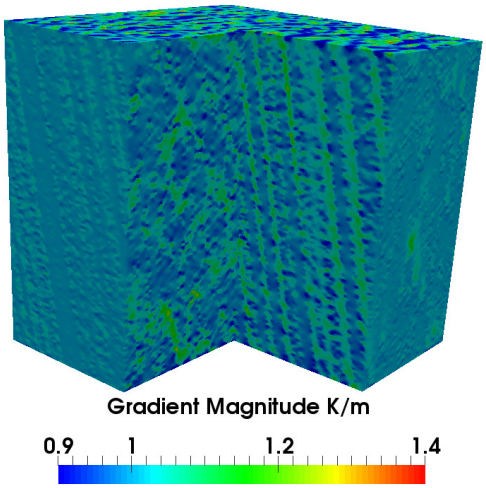

FIGURE 5 – Temperature gradient of E–glass fibers in composite

ROI of the GFRP is :

$$\boldsymbol{A_c} = \left\{\begin{array}{ccc} 0.625 & 0.002 & -0.002 \\ 0.002 & 0.629 & 0.025 \\ -0.002 & 0.025 & 0.745 \end{array}\right\} W/(mK)$$

which confirms that GFRP is an orthotropic material. This effective property tensor is for the fibers with an orientation of $-15°$, for that of the $+15°$ orientation, one can derive it directly.

3.4 Large simulation from a X-Ray tomographic image

The applications introduced above reveal that, the effective conductivity can be obtained by numerical simulation directly from an X-Ray tomographic image, without any human intervention. The current tomographic images have $2048 \times 2048 \times 2048$ voxels or more than 8 billion elements. The final application for this work it to carry out the numerical simulation with such a large image.

The image used in this case is the GFRP image of the previous application. One takes a part from the original image, the ROI consists of 513^3 voxels. As presented in Figure 6, it consists of four layers with different E–glass fiber orientations. One employs a two times sub-sampling to obtain an image consisting of 2048^3 elements. The smoothing process on gray level is also applied and the material property has been assigned to each node as presented in Figure 6.

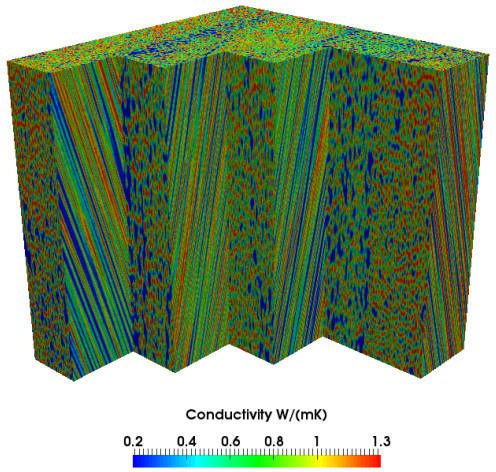

FIGURE 6 – E–glass fiber orientation in each layer and conductivity at each elementary node

768 cores (64 MPI, 12 OpenMP/MPI) are used simultaneously. The calculation time is four hours. Figure 7 illustrates the residual evolution with the number of MG V-Cycles. Regardless of the size of the problem, the convergence remains very good. To achieve a residual of 10^{-6}, only 9 MG V-Cycles are needed. It means that the number of relaxations on the finest level is only 27. It confirms the efficiency of the strategy used in this work. The temperature gradient is presented in Figure 8. Figure 8 and 9 illustrate

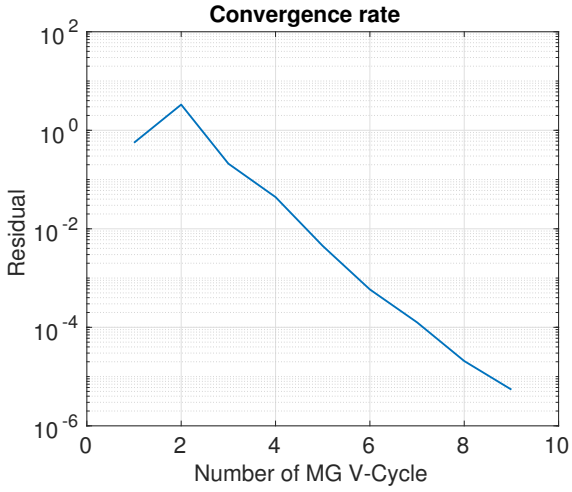

FIGURE 7 – Convergence

the correspondence between conductivity and temperature gradient.

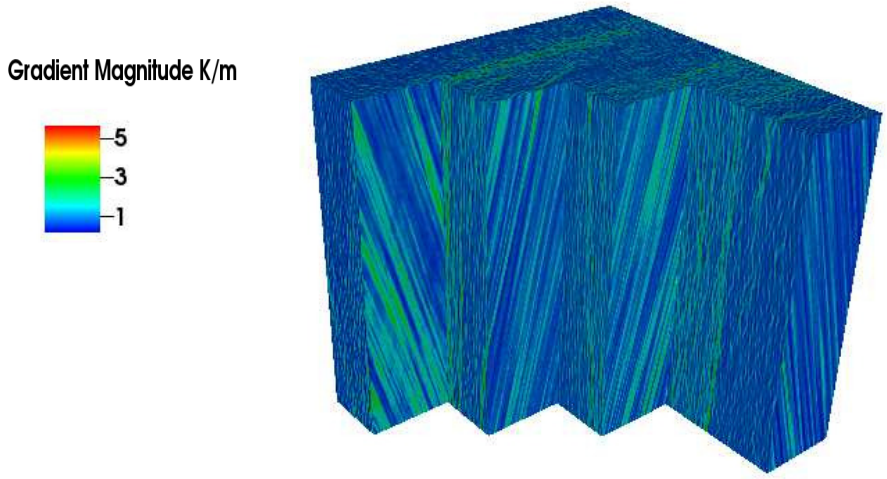

FIGURE 8 – Temperature gradient

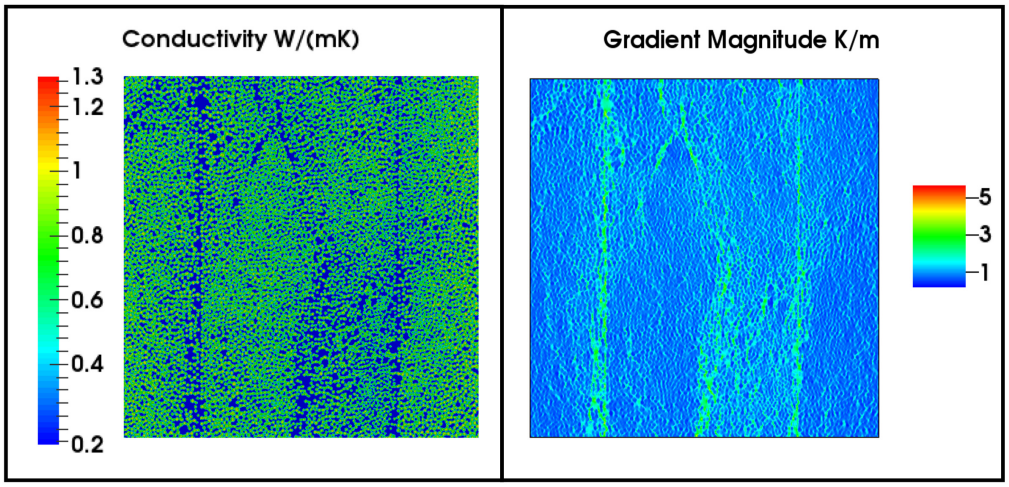

FIGURE 9 – Conductivity (Left) and temperature gradient (Right)

4 Discussion and Conclusions

The aim of this paper is to present that one can employ numerical simulations directly on large tomographic images. To perform the simulations with such a large number of elements and such large variations of materials properties requires dedicated algorithms and hardware. The strategy to use the MG method coupled with a homogenization technique, permits one to deal with this kind of problems. The applications and numerical comparison presented above demonstrate the efficiency of the MG method. The homogenization technique shows its capacity to increase the stability of the MG scheme, when large variations of materials properties exits. The Matrix Free FEM demonstrate its good performance for large problems up to 8 billion of elements. The strategy to apply one voxel per elementary node avoids human intervention. The effective material property can be automatically obtained by using the large X-Ray tomographic image, as an input, without complex experimental measurement. The Hybrid MPI/OpenMP programming shows its good feasibility and performance for the MG method.

The thermal conductivity is analyzed in this work. In future work, the mechanical property of materials will be analyzed. The property at each node is supposed to be isotropic, additional research is needed for the anisotropic case.

Acknowledgments

The support of Région Pays de la Loire and Nantes Métropole through a grant Connect Talent IDS is gratefully acknowledged.

Références

[1] Brian P Flannery, Harry W Deckman, Wayne G Roberge, and KEVIN L D'AMICO. Three-dimensional x-ray microtomography. *Science*, 237(4821) :1439–1444, 1987.

[2] Mea Lengsfeld, J Schmitt, P Alter, J Kaminsky, and R Leppek. Comparison of geometry-based and ct voxel-based finite element modelling and experimental validation. *Medical engineering & physics*, 20(7) :515–522, 1998.

[3] Masahiko Bessho, Isao Ohnishi, Juntaro Matsuyama, Takuya Matsumoto, Kazuhiro Imai, and Kozo Nakamura. Prediction of strength and strain of the proximal femur by a ct-based finite element method. *Journal of biomechanics*, 40(8) :1745–1753, 2007.

[4] Matthieu Ferrant, Simon K Warfield, Charles RG Guttmann, Robert V Mulkern, Ferenc A Jolesz, and Ron Kikinis. 3d image matching using a finite element based elastic deformation model. In *International Conference on Medical Image Computing and Computer-Assisted Intervention*, pages 202–209. Springer, 1999.

[5] N Michailidis, F Stergioudi, H Omar, and DN Tsipas. An image-based reconstruction of the 3d geometry of an al open-cell foam and fem modeling of the material response. *Mechanics of Materials*, 42(2) :142–147, 2010.

[6] Henry Proudhon, Jia Li, F Wang, A Roos, Vincent Chiaruttini, and Samuel Forest. 3d simulation of short fatigue crack propagation by finite element crystal plasticity and remeshing. *International Journal of Fatigue*, 82 :238–246, 2016.

[7] Hanfeng Gu, Julien Réthoré, Marie-Christine Baietto, Philippe Sainsot, Pauline Lecomte-Grosbras, Cornelis H Venner, and Antonius A Lubrecht. An efficient multigrid solver for the 3d simulation of composite materials. *Computational materials science*, 112 :230–237, 2016.

[8] Graham F Carey and Bo-Nan Jiang. Element-by-element linear and nonlinear solution schemes. *Communications in Applied Numerical Methods*, 2(2) :145–153, 1986.

[9] RE Alcouffe, Achi Brandt, JE Dendy, Jr, and JW Painter. The multi-grid method for the diffusion equation with strongly discontinuous coefficients. *SIAM Journal on Scientific and Statistical Computing*, 2(4) :430–454, 1981.

[10] Rudi Hoekema, Kees Venner, Johannes J Struijk, and Jan Holsheimer. Multigrid solution of the potential field in modeling electrical nerve stimulation. *Computers and Biomedical Research*, 31(5) :348–362, 1998.

[11] Bjorn Engquist and Erding Luo. New coarse grid operators for highly oscillatory coefficient elliptic problems. *Journal of Computational Physics*, 129(2) :296–306, 1996.

[12] Bjorn Engquist and Erding Luo. Convergence of a multigrid method for elliptic equations with highly oscillatory coefficients. *SIAM journal on numerical analysis*, 34(6) :2254–2273, 1997.

[13] Rosangela F Sviercoski, Peter Popov, and Svetozar Margenov. An analytical coarse grid operator applied to a multiscale multigrid method. *Journal of Computational and Applied Mathematics*, 287 :207–219, 2015.

[14] Pauline Lecomte-Grosbras, Julien Réthoré, Nathalie Limodin, J-F Witz, and Mathias Brieu. Three-dimensional investigation of free-edge effects in laminate composites using x-ray tomography and digital volume correlation. *Experimental Mechanics*, 55(1) :301–311, 2015.